J. Membrane Biol. 111, 37–48 (1989)

The Journal of
Membrane Biology

Fusion of Cultured Dog Kidney (MDCK) Cells: I. Technique, Fate of Plasma Membranes and of Cell Nuclei

Ulrich Kersting, Heribert Joha, Wieland Steigner, Birgit Gassner, Gerhard Gstraunthaler†, Walter Pfaller†, and Hans Oberleithner

Department of Physiology, University of Würzburg, D-8700 Würzburg, Federal Republic of Germany and †Department of Physiology, University of Innsbruck, A-6010 Innsbruck, Austria

Summary. The evaluation of the intracellular signal train and its regulatory function in controlling transepithelial transport with electrophysiological methods often requires intracellular measurements with microelectrodes. However, multiple impalements in epithelial cells are hampered by the small size of the cells. In an attempt to avoid these problems we fused cells of an established cell line, Madin Darby canine kidney cells, originally derived from dog kidney, to "giant" cells by applying a modified polyethylene glycol method. During trypsin-induced detachment from the ground of the petri dish, individual cells grown in a monolayer incorporate volume and mainly lose basolateral plasma membrane by extrusion. By isovolumetric cell-to-cell fusion, spherical "giant" cells are formed within 2 hr. During this process a major part of the individual cell plasma membranes is internalized. Over three weeks following cell plasma membrane fusion degradation of single cell nuclei and cell nuclear fusion occurs. We conclude that this experimental approach opens the possibility to investigate ion transport of epithelia in culture by somatic cell genetic techniques.

Key Words Cell membrane fusion · cell nuclei fusion · cell culture · MDCK cells · lectins · acridine orange

Introduction

In the past the application of electrophysiological techniques has led to an enormous progress in the understanding of kidney function and kidney disease [4, 7, 8, 37]. In the last ten years renal physiologists focused their investigations on studying renal transport at the cellular level, for example, elucidating the intracellular signal train and its regulatory function in transepithelial transport. Intracellular impalements with microelectrodes, microinjections, patch clamp or cell culture techniques were used increasingly to characterize transmembrane ion transport. However, the application of ion-selective microelectrodes and intracellular impalements with more than one microelectrode were still hampered by the small size of renal epithelial cells. To overcome this problem we have fused single renal cells from the frog to giant cells [6, 22]. In these giant cells stable measurements with several microelectrodes were feasible over long periods [34]. Recently, cells from the proximal convoluted tubule of *Necturus* kidney have been fused successfully with this fusion method [3]. So far, the fused cells of frog kidney have served as a model to study aldosterone action [23] and acid-base transport at the cellular level [6, 34].

In the present paper we will describe a method to fuse single cultured cells to giant cells. We have chosen epithelial cells from the dog kidney (Madin Darby canine kidney cells, MDCK) [18]. This cell line is well examined by physiologists and cell biologists [5, 10, 20, 24, 25, 27, 30, 33]. A major advantage of culture cells over native tissue is that cloned cells grow under well-controlled conditions and can be harvested in large amounts. In Materials and Methods we present detailed instructions on how to fuse single cells obtained from cell culture to giant cells. In Results we discuss the fate of single cell membranes and single cell nuclei during trypsination and fusion. We also present evidence based on electron microscopy that plasma membrane is internalized in the process of cell-to-cell fusion. Finally, in the Discussion some future aspects of epithelial fusion are addressed.

Materials and Methods

Method of Cell Fusion

For cell-to-cell fusion we have chosen the polyethylene glycol (PEG) method [16, 26, 35]. Another frequently used fusion

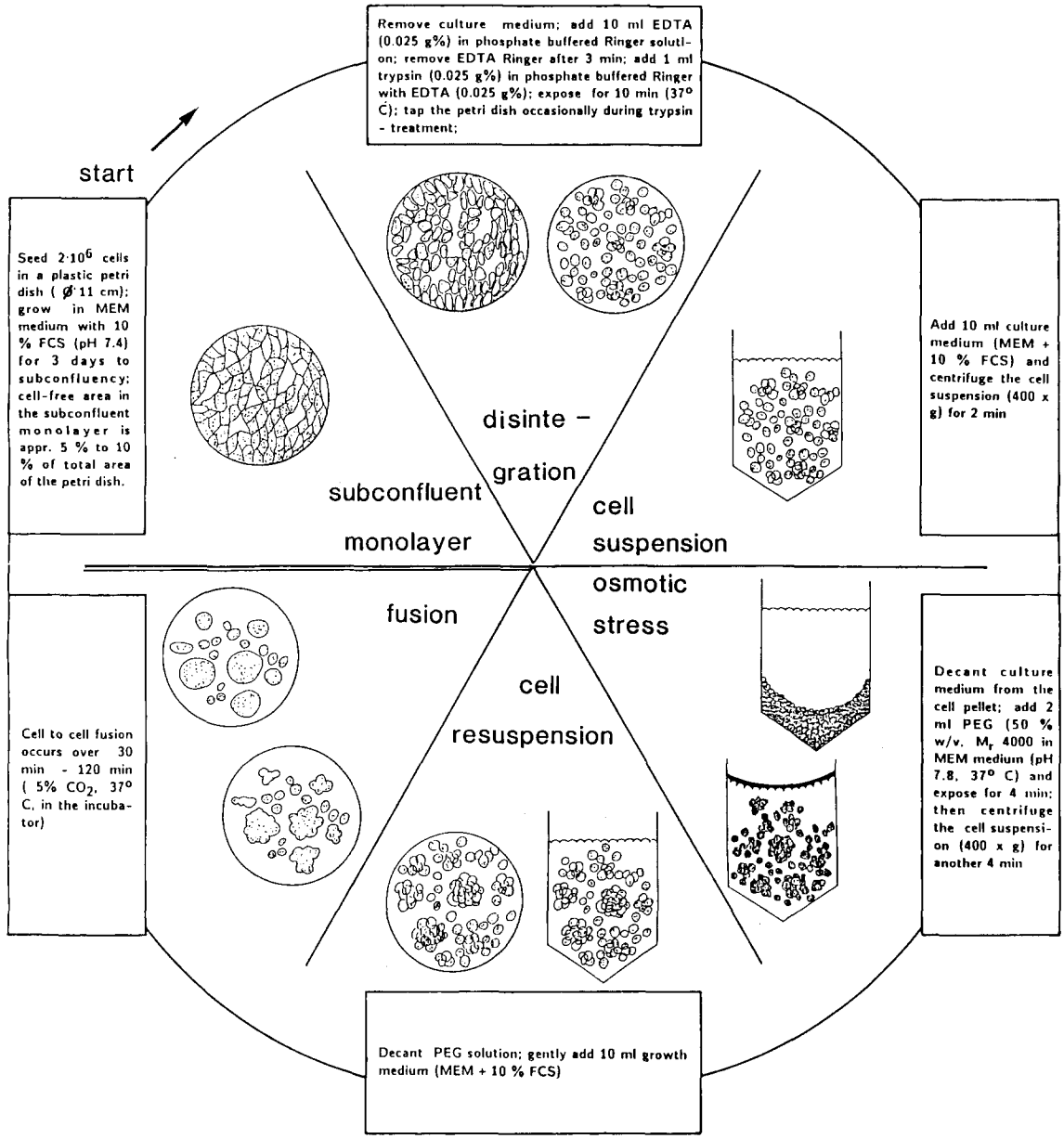

Fig. 1. Technical aspects of cell-to-cell fusion

method is the electric field-induced fusion technique [38]. The crucial point of the PEG method is the application of an osmotic stress to initiate membrane fusion. We hope that the laboratory instructions described in this chapter in detail lead also to successful fusions with other cell types. All steps of the fusion method are summarized in a schematic drawing (Fig. 1).

Cell Growth in a Subconfluent Monolayer

About 2×10^6 MDCK cells were seeded in dry coated plastic culture flasks (growth area = 75 cm^2; Nunc, Wiesbaden, FRG) in 10 ml Minimum Essential Medium with Earle's salts, nonessentiell amino-acids and L-glutaminic acid (MEM medium, Biochrom KG, Berlin, FRG). The MEM medium was supplemented with 10% fetal calf serum (Biochrom KG, Berlin, FRG) and 26 mmol/liter $NaHCO_3$. Cells were grown at 37°C in a 5% CO_2 in air, humidified atmosphere. Four days later cells were harvested by trypsin treatment (*see* below) and split. 2×10^6 cells were again seeded in a culture flask, whereas another 2×10^6 cells were plated onto a dry coated plastic petri dish (diameter = 8.5 cm, Nunc, Wiesbaden, FRG). In the fusion experiments we have fused cells from the 68th to 90th passage. We recommend not to use cells with a passage number beyond 90, because fusion experiments with these cells result in smaller and less-vital fused cells. For the cell-to-cell fusion we used the cells harvested from the plastic petri dish grown to a subconfluent monolayer three days later. The cell density in this growth phase was ca. 10^6 cells/

cm^2. Approximately 5 to 10% of the total area of the petri dish were cell-free islands. We want to emphasize that the specific growth phase of the single cells is very important for successful cell fusion. Fusion of cells from a "young" subconfluent layer, perhaps harvested 2 days after plating, results in large fused cells with reduced vitality. Fusion of cells from an "old" confluent monolayer results in small and also less-vital cells. One reason for this reduced vitality may be the prolonged duration of the trypsination procedure necessary to disrupt the "old" confluent monolayer.

Disintegration of the Subconfluent Monolayer

Cells grown in a subconfluent monolayer were isolated by trypsination. For this purpose we removed the culture medium and washed the monolayer with 10 ml of a Ca^{2+} free, EDTA-containing solution. The EDTA solution was composed of (mmol/liter): 0.67 EDTA, 137 NaCl, 2.7 KCl, 6.5 Na_2HPO_4, 1.5 KH_2PO_4, pH 7.4. With this procedure the junctional complexes are broken and cells will lose cell-to-cell contact [20, 28]. Then we added 1 ml trypsin (40 U/mg, 0.025 g%) in Ca^{2+} free, EDTA solution (*see* above) to the subconfluent monolayer. In the Ca^{2+} free solution trypsin can move freely between the cells to the basolateral cell membrane surface still attached to the bottom of the petri dish. Trypsination was accelerated by increasing the temperature to 37°C and cell detachment was supported by occasional tapping of the petri dish. The duration of the trypsin treatment is an important point in the fusion process. Long duration of trypsin treatment (e.g., 20 min) increases the fusion capacity of the single cells, resulting in large yet less-vital cells. Therefore we limited the duration of trypsin treatment. As a major criterion, we stopped trypsination when about 75% of the cells in the petri dish were isolated. At this stage, small cell-to-cell aggregations become visible. The cell diameter of a single spherical cell after trypsination was 17.4 ± 2.1 μm (M ± SEM, n = 63), (Fig. 2A). Spherical cells with diameters up to 40 μm could also be detected. These rather large cells showed only one nucleus and therefore seemed to be single and not spontaneously fused cells. Trypsination was stopped by adding 10 ml culture medium to the trypsin solution. Then we centrifuged the cell suspension (400 × g) for 2 min. The culture medium was decanted and cell-to-cell fusion was started by the gentle addition of polyethylene glycol to the cell pellet. For our photographic studies (Kodak Ektachrome 50 Professional Film) the cells were suspended in HEPES-buffered Ringer's solution and transferred on a thin microscope glass coverslip. The Ringer's solution was composed of (mmol/liter): 130 NaCl, 5.4 KCl, 1.2 $CaCl_2$, 0.8 $MgCl_2$, 10 HEPES, 5.5 glucose, pH 7.4. We used differential interference contrast microscopy (DIC), (inverted microscope, IM 35 (Fa. Zeiss, Oberkochen, FRG), objective lens 40/0.65 or 63/1.4, oil).

Application of an Osmotic Stress

Two ml of the polyethylene glycol solution (50% wt/vol PEG, M_r 4000, in MEM culture medium without calf serum, pH 7.8, 37°C) was added slowly to the cell pellet and the cells were gently suspended. In the PEG suspension cell shrink and close plasma membrane contact between adjacent cell occurs [15]. Large cell aggregations with up to several hundred single cells can be detected during PEG treatment (Fig. 2*B*). From these grape-like plaques the fused cells will be formed later. After 4 min the PEG suspension was centrifuged (400 × g, for another 4 min). Then the cells were resuspended in culture medium with 10% fetal calf serum. The grape-like plaques do not disappear during this reswelling procedure (Fig. 2*C*). The cells remain in close contact to each other after removal of PEG [15]. The process of cell swelling initiates plasma membrane fusion in these plaques by establishing small cytoplasmic connections.

Plasma Membrane Fusion of MDCK Cells

The cell aggregations were kept incubated over a range of 30 to 120 min after PEG treatment in plastic petri dishes (37°C, 5% CO_2, pH 7.4). During this time period membrane fusion occurs, single cell borders disappear (Fig. 2*D*), and round-shaped spherical cells are formed (Fig. 2*E*). We found approximately 100 "giant" cells with diameters between 60–80 μm per petri dish. After complete plasma membrane fusion the cells were transferred onto a thin microscope coverslip pretreated with poly-L-lysin (0.1 mg/ml (Serva, Heidelberg, FRG)). Then the fused cells were ready for electrophysiological studies using differential interference contrast microscopy. To demonstrate that the cytoplasmic compartment in the fused cells was homogeneous, we used intracellular iontophoretic injections of the fluorescence dye Lucifer yellow (100 mmol/liter in H_2O (Fluka, Neu Ulm, FRG); Fig. 2*F*) [32]. Some specific physiological properties of the fused MDCK cells will be presented in the subsequent paper [21].

During trypsination, i.e., when the cell shape changes from flat to spherical, an alteration of cell volume-to-surface ratio is expected. Furthermore, proposing isovolumetric cell-to-cell fusion, there must be loss and/or degradation of plasma membrane. In a fused cell many single-cell nuclei must exist shortly after fusion. To further investigate the fate of the individual plasma membranes and cell nuclei in the fused cells we marked single-cell membranes with fluorescence-labeled lectins and stained single-cell nuclei with the fluorescent dye acridine orange.

Results

Fate of Individual Plasma Membranes and Cell Nuclei during Trypsination and Cell-to-Cell Fusion

Alteration of the Volume-to-Surface Ratio during Trypsination

To address this issue we observed six adjacent cells during trypsination using differential interference contrast microscopy (Fig. 3). In Fig. 3*A* a subconfluent monolayer with a cell-free island (*X*) is shown. We estimated the cell membrane surface of a single cell in the subconfluent monolayer from the visible surface of the six cells shown in Fig. 3*B*. For our calculations we neglected luminal microvilli and basolateral membrane enfoldings according to the observation that on microscope coverslips hardly any folds are visible in MDCK cells 6 days after plating [14]. Nevertheless, there may be still some plasma membrane enfoldings in the luminal and

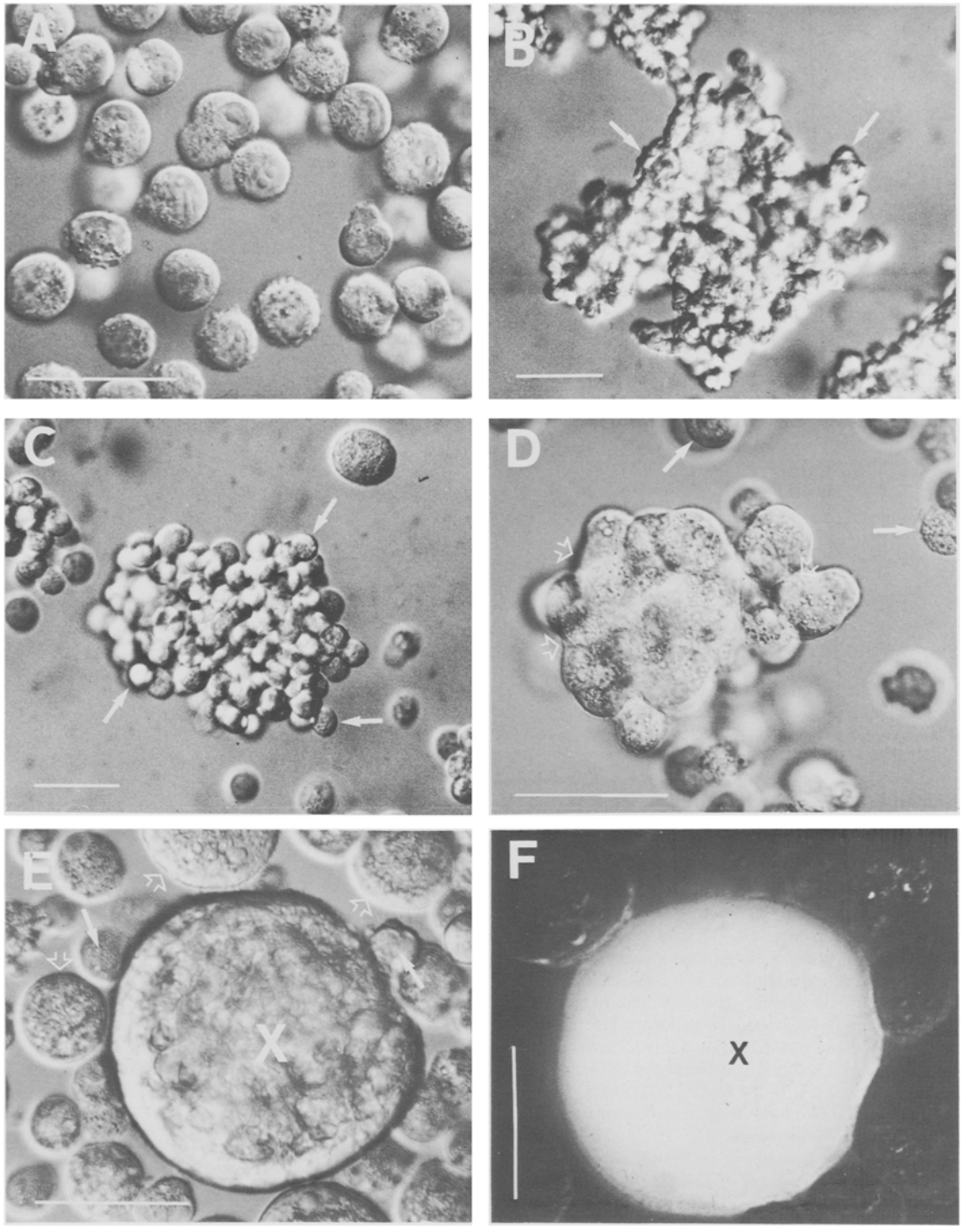

Fig. 2. Fusion of MDCK cells. The bars indicate a length of 50 μm. (*A*) Spherical cells after trypsination. (*B*) Cell aggregation in polyethylene glycol (PEG). Cells are extremely dehydrated and cell borders hardly visible (arrows). (*C*) Cell aggregation in medium immediately after removal of PEG. Cells are rehydrated and clearly visible. (*D*) Cell aggregation in medium 30 min after PEG treatment. Single-cell borders disappear and the uniform outer plasma membrane starts to develop (open arrows). Two single cells are marked with solid arrows. (*E*) Fused spherical cell 120 min after PEG treatment (X). Single cells are marked with solid arrows and small fused cells with open arrows. (*F*) The same fused cell a few seconds after injection of the fluorescence dye Lucifer yellow

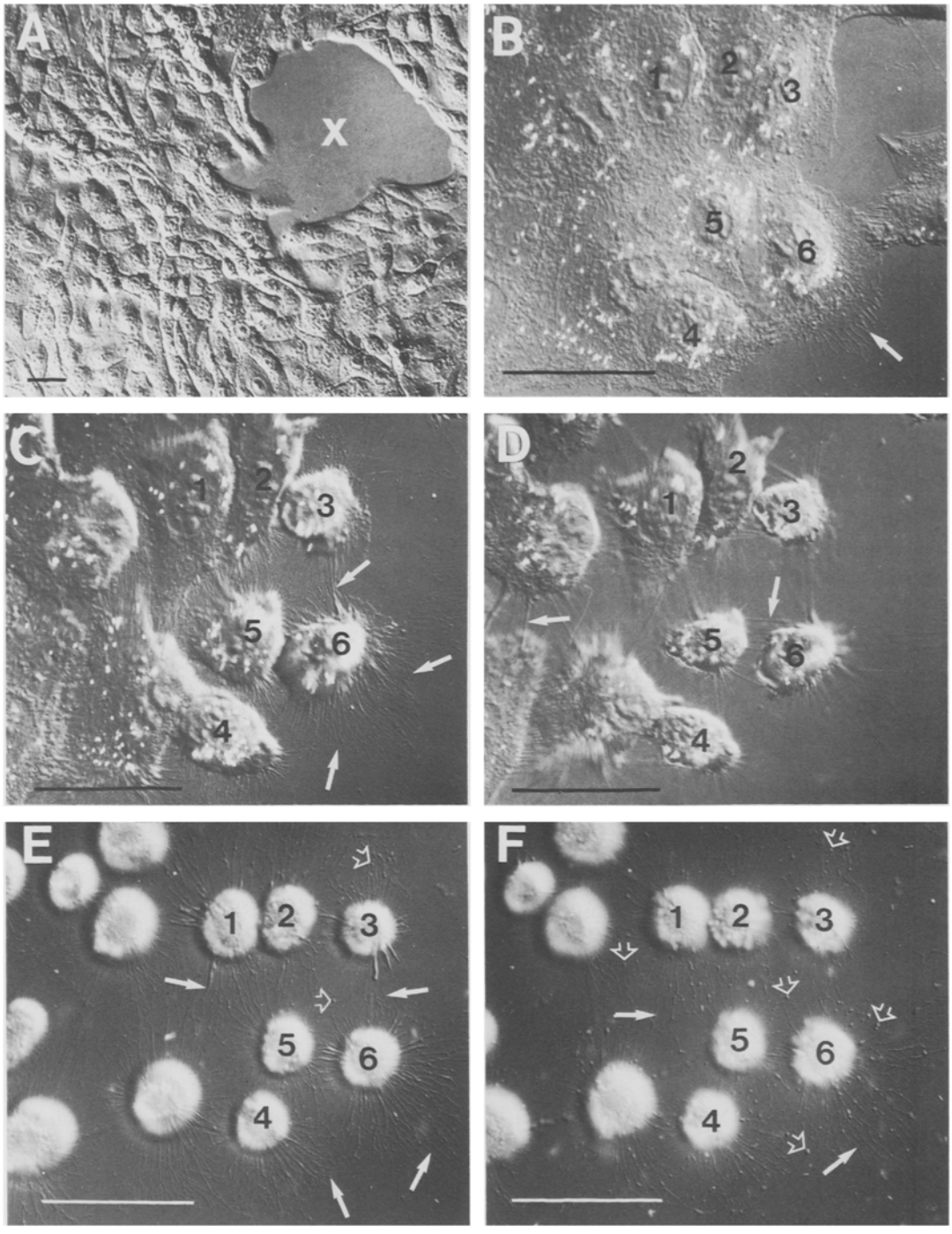

Fig. 3. Trypsination of a subconfluent monolayer of MDCK cells. The bars indicate a length of 50 μm. Numbers *1–6* correspond to the same cells (*B–F*). (*A*) Subconfluent monolayer with a cell-free island (X). (*B*) Edge of the monolayer close to the cell-free island. From the cells *1–6*, cell surface was determined (*see* text). The solid arrow indicates membrane fibers. (*C*) Cells 2 min after application of trypsin. Gaps appear between cells. Fiber network of cell material covers the glass surface (arrows). (*D*) 4 min trypsin. Strings (arrows) directly connect trypsinated cells; upper focus level. (*E*) 10 min trypsin. The glass surface is covered with a fiber network (solid arrows). Additionally, small vesicles appear (open arrows). (*F*) 25 min trypsin. A large number of individual fibers (solid arrows) has been transformed into vesicles (open arrows)

basolateral membrane and thus we will rather underestimate the correct total cell membrane surface. Furthermore, for the calculation of the cell membrane surface the height of the cells can be neglected. High resolution interference contrast microscopy allows optical sectioning of the cells (DIC, objective 63/1.4, oil (Fa. Zeiss, Oberkochen, FRG)) [31] and thus determination of cell height. In the subconfluent monolayer cell height was smaller than 1 μm. In confluent monolayers, 6 days after plating, cells grown on similar supports have thicknesses of 3–5 μm in the cell center and 0.2 μm in the cell periphery [14]. Based on the cells displayed in Fig. 3 we calculate a cell membrane surface of a single cell in the subconfluent monolayer of approximately 1800 μm^2. The cell volume of a single cell was calculated to be 900 μm^3, assuming a cell height of 1 μm. This value is rather an overestimation of the true cell volume of single cells in a subconfluent monolayer. After trypsination the cells become spherical and cell surface and cell volume can be calculated easily from the radius of the cells. The mean radius of six spherical cells (Fig. 3*F*) was 9.2 μm and thus surface was 1070 μm^2 and cell volume was 3260 μm^3. These values indicate that during trypsination more than 40% of single cell membrane surface disappear and that cells must dramatically incorporate volume during detachment from the ground of the culture dish. The question arises whether plasma membrane is either extruded or internalized. It will be shown later that in cells with fluorescence-labeled cell membranes the marker was found only in the plasma membrane of the trypsinized spherical cells but not in the cytoplasmic compartment. Thus an internalization of plasma membrane during trypsination seems unlikely.

Figure 3*C–F* shows the time course of trypsination using high resolution interference contrast microscopy. Cells were grown on microscope coverslips and were trypsinized at room temperature with the same procedure as described in Materials and Methods. Prior to trypsin treatment cells are still flat (Fig. 3*A*; low magnification) and cell borders are hardly visible (Fig. 3*B*; high magnification). Focused at the solid glass surface one can notice cell structures protruding into the cell-free space (Fig. 3*B*; solid arrow). Two minutes after application of trypsin (Fig. 3*C*) gaps can be disclosed between cells, while cells become spherical. This process starts first in cells close to the cell-free islands (Fig. 3*C*; right part).

However, while changing shape the cells are still connected to each other with many cobweb-like strings (Fig. 3*D*; solid arrows). Fig. 3*D* shows the same cells 4 min after addition of trypsin, now focused at a higher level. The solid arrows indicate direct cell-to-cell connections, which often swing freely without any contact to the glass surface. 10 min after initiation of trypsin treatment cells have reached a spherical shape while the cell-free space is now covered with a fiber network of nonidentified cell material (Fig. 3*E*; solid arrows, focused on the glass surface). Additionally, some small vesicles become visible (open arrows). Over the following minutes, an increasing number of strings turns into vesicles, as shown in Fig. 3*F* (25 min after trypsin application). The formation of strings, fibers and vesicles indicates that at least part of the cell surface is externalized during the process of trypsination.

Due to the fact that growing cells are attached to the solid support with their basolateral plasma membranes, it is likely that the membrane lost during the process of trypsination is mainly of basolateral origin. Thus a significant amount of specifically basolateral transport proteins (e.g., ion pumps and ion channels) could have disappeared during trypsination. However, due to the lack of differentiation of MDCK cells when grown on glass or plastic [14, 29], we can assume that there are still basolateral transport proteins remaining in the plasma membrane of the spherical cell, even though 40% of the total membrane is eliminated.

Alteration of the Volume-to-Surface Ratio during Cell-to-Cell Fusion

When a spherical fused cell is viewed under the microscope with a high resolution objective lens (63/1.4, oil) [31], the depth of field is shallow. Thus it is possible to cut the cytoplasmic compartment in thin optical slices and to estimate the number of nuclei in fused cells. Each single nucleus originates from an individual cell. Then the number of single cells fused to form a "giant" cell can be determined. We also calculated the volume of a single cell and the volume of the fused cell from their respective radii. The sum of the single cell volumes was in the range of the cell volume of an individual fused cell. Theoretically, 20 individual cells with a mean single cell radius of 8.7 μm and a single cell volume of 2,483 μm^3 will fuse to a giant cell with a volume of 49,654 μm^3, proposing an isovolumetric fusion process. Experimenally, we counted 20 single-cell nuclei in a fused cell with a radius of 23 μm and a cell volume of 50,965 μm^3. Therefore, we assume isovolumetric cell-to-cell fusion. Based on this assumption, about 40 single cells are necessary to form one giant cell with a diameter of 60 μm, thereby losing 70% of the plasma membrane surface.

In order to study the fate of the plasma mem-

brane in more detail, we marked the plasma membranes of single cells with fluorescence labels before fusion. After trypsin treatment the single cells were either exposed to FITC-labeled or to Rhodamine-labeled peanut lectins (both peanut lectins were purchased from Medac, Hamburg, FRG; incubation of the cells in 100 μg/ml peanut lectin in HEPES Ringer for 30 min, room temperature) [13, 17]. Figure 4*A* shows a mixture of cells with either one of the two labels using DIC microscopy. The same cells are shown in Fig. 4*B*, now in a double exposure to two different excitation wave-lengths (FITC label visible at 450 to 490 nm and Rhodamine label visible at 510–560 nm) in the fluorescence microscope. In Fig. 4*A* and *B* Rhodamine-labeled cells are visible (solid arrows) as well as FITC-labeled cells (open arrows). In an incompletely fused cell, about 30 min after PEG treatment, cell membranes of single cells are still visible (Fig. 4*C–E*). 120 min after initiation of cell-to-cell fusion plasma membranes of individual cells become increasingly disrupted (Fig. 4*E*). Since Rhodamine-labeled (red) membranes and FITC-labeled (green) membranes mix, the two wavelengths add and a yellowish color will stain the cytoplasmic compartment. In a completely fused cell 2 hr after PEG treatment (Fig. 4*F*) single-cell membranes are no longer visible. In this giant cell both markers are dispersed all over in the cytoplasmic compartment. These observations indicate that a major portion of single-cell membrane is internalized during cell membrane fusion. Surprisingly, the membrane markers cannot be detected in the plasma membrane of the giant cell. An explanation may be that a major portion of peanut-labeled glycoproteins is internalized during the process of fusion and thus not detectable in the plasma membrane of the fused cell. However, binding sites for peanut lectins must exist because cells fused from unlabeled single cells can be successfully labeled with peanut lectins two hours after fusion (*unpublished observation*, our laboratory). Electron microscopy reveals that there are indeed single-cell membrane markers visible in the plasma membrane of the fused cells two hours after PEG treatment (*see* below). We assume that a major portion of glycoproteins disappears from the fused plasma membrane, possibly by metabolic turnover, and that the fraction of peanut lectins bound to glycoproteins remaining in the plasma membrane is too small to be detected by fluorescence microscopy.

Fate of Cell Nuclei after Plasma Membrane Fusion

Fused cells attach immediately to a poly-L-lysine coated microscope glass coverslip. They remain approximately spherical over several hours. 24 hours after plating cells have changed their shape from spherical to flat. To further investigate the fate of the fused multinucleated cells, the cell nuclei of flat cells were stained with the fluorescent dye acridine orange (100 μg/ml in HEPES solution). Flat cells on a coverslip were exposed for 1 min to the acridine orange solution at different times after PEG treatment (in days: 1, 7, 10, 21). Then the cells were washed with the normal Ringer's solution and photographed. We wanted to observe cell nuclear fusion in an individual fused cell. Unfortunately, cell growth and cell division are inhibited by this fluorescent dye. Thus we were not able to observe nuclear fusion and finally cell division of an individual multinucleated homokaryon over several days or weeks. The inhibitory action can be explained by the fact that acridine orange is a potent inhibitor of protein kinase C [11]. This plasma membrane-associated enzyme plays, indeed, a major role in cell growth and mitosis [2]. Therefore, in an unpaired study we observed changes in shape and number of cell nuclei in multinucleated homokaryons grown on several coverslips over a time course of weeks after fusion. Single cells (one nucleus) and a large number of small fused cells (more than one nucleus) stick to the glass coverslip 24 hours after fusion (Fig. 5*A*). The diameter of a single cell nucleus in a cell of a subconfluent monlayer is 17.7 $\pm$ 1.5 μm (mean $\pm$ SEM, $n = 33$). Usually we found on a single coverslip (diameter 25 mm) 1 day after PEG treatment about 10 multinucleated homokaryons with more than 20 nuclei (Fig. 5*B*). The nuclei in the giant cells are more or less round shaped and initially similar in size as compared to the nuclei of single cells. 21 days after cell membrane fusion there are still giant cells detectable but cells are not polynucleated anymore (Fig. 5*E*). They have only one rather large nucleus with a diameter of about 44 μm (i.e., two- to threefold the normal nucleus). Cells with such large nuclei cannot be detected three weeks after single (nonfused) cells were plated. Intermittent observations at different times after fusion reveal (Fig. 5*C* and *D*) that the number of nuclei decreases continuously whereas the size of the remaining nuclei increases. Furthermore, about a week after fusion the outlines of the nuclei become irregular and configurations of nuclear fusion occur frequently. From these observations we conclude that with a lag period of about one week after plasma membrane fusion cell nuclei are either degradated or fused to each other. Cell nuclear fusion was already performed experimentally in 1965 and heterokaryons of mammalian cells from different species were formed [12]. In the present study we have fused single cells to large homokaryons in order to study the process of fusion and to establish

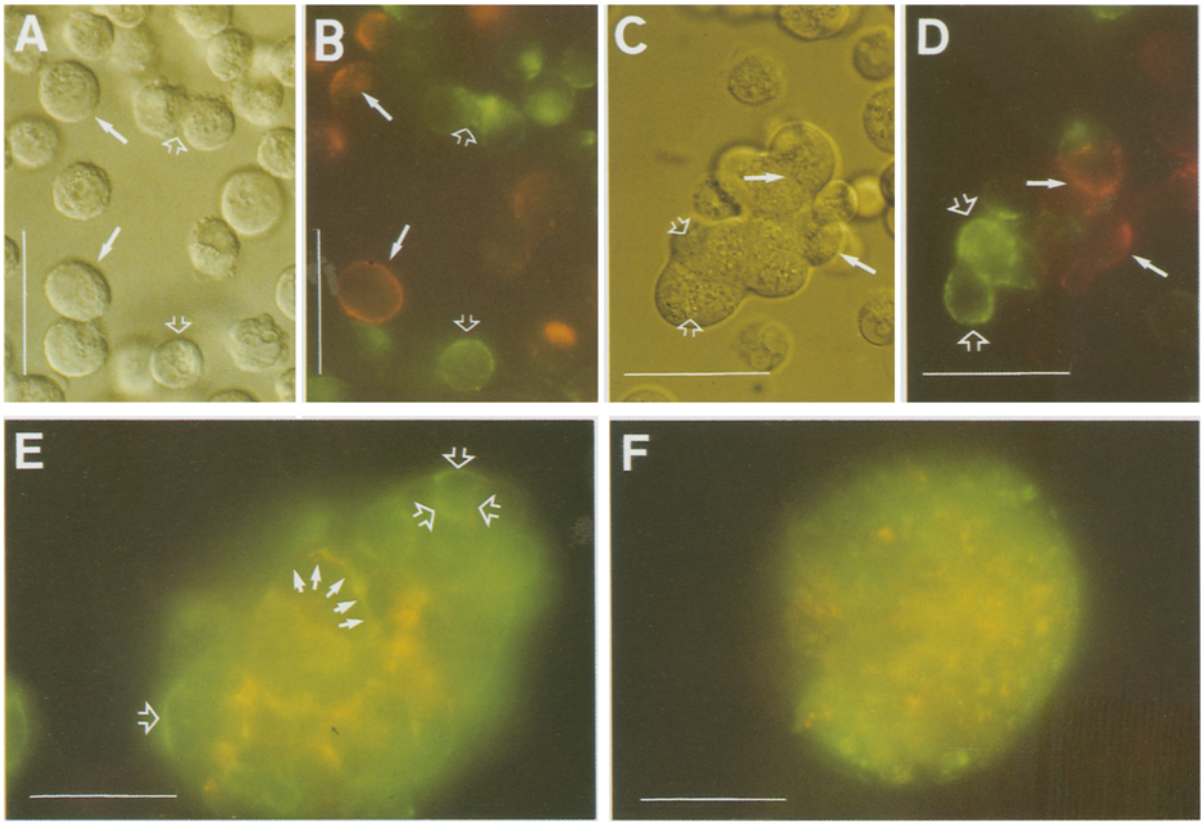

Fig. 4

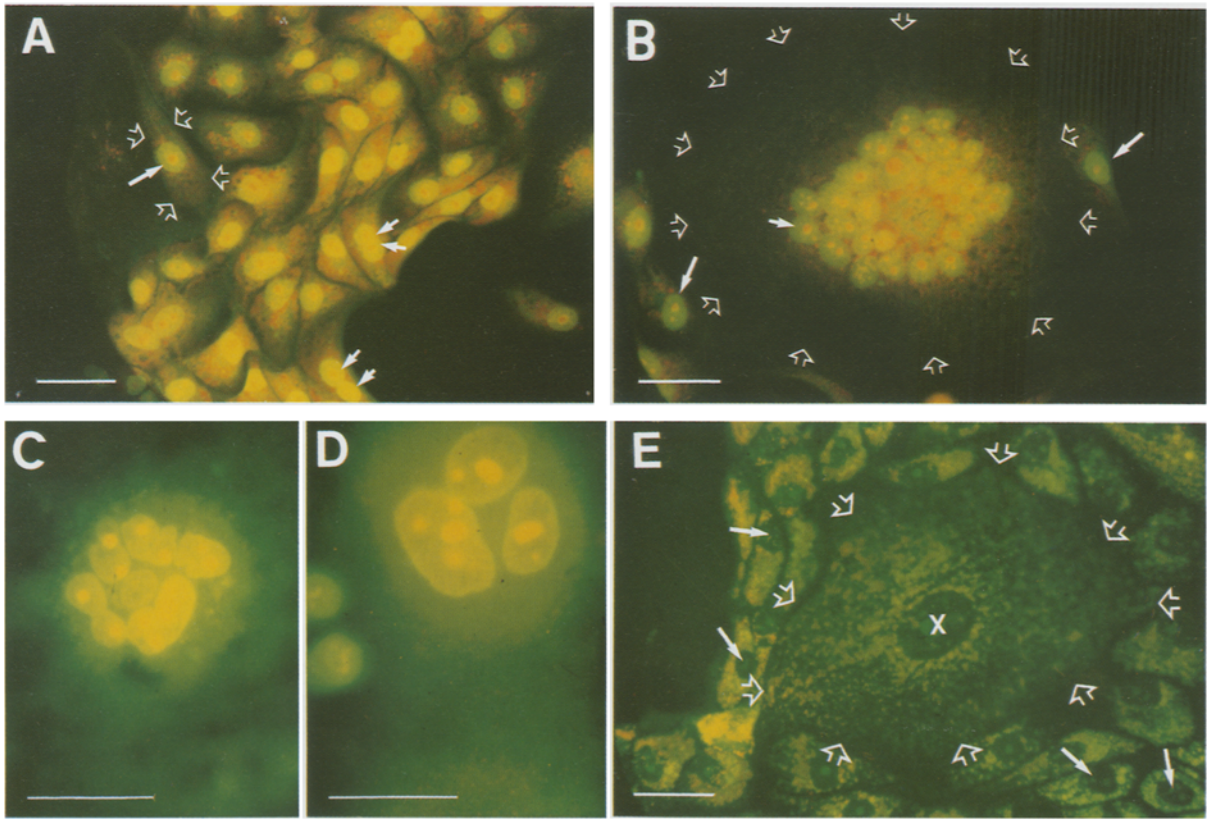

Fig. 5

a biological model in which extensive intracellular manipulations should be feasible.

Electron Microscopy of Polynucleated Homokaryons

Again, plasma membranes of two patches of individual single cells obtained from MDCK monolayers were labeled with two different lectins and fused. Then we looked for the labels by electron microscopy.

Method of Plasma Membrane Labeling

A cell supension of MDCK cells was split into two groups. One set was incubated for 30 min at 4°C in PBS containing 16.2 mg/ml concanavalin A covalently coupled to colloidal gold (Con A-gold, Polysciences, Warrinton, PA). The other set was labeled with 450 μg/ml of succinylated Con A conjugated to ferritin (succinyl Con A-ferritin, Polysciences). In a parallel series of experiments, two sets of MDCK cells were labeled with 830 μg/ml peanut lectin coupled to horseradish peroxidase (PNA-HRP, Biomaker, Rehovot, Israel) and succinyl Con A-ferritin, respectively.

The two different labeled cell populations were then washed two times with PBS containing Ca^{2+} and Mg^{2+} and combined for cell fusion with PEG. After fusion and addition of fresh culture medium the lectin-labeled cells were incubated in suspension for 2 hr at 37°C. Thereafter the cell suspensions were centrifuged and fixed with 1% glutaraldehyde buffered with sodium-cacodylate (pH 7.4) at 4°C for 1 hr, washed with cacodylate-buffer, incubated with 3,3-diaminobenzidine [9], postfixed in 1% OsO_4 containing 1.5% $K_4Fe(CN)_6$ [36], and 1% tannic acid in cacodylate-buffer, dehydrated in graded series of acetone, and embedded in araldite (Durcupan ACM, Fluka, Switzerland). Staining of ultrathin sections of all preparations was performed with bismut subnitrate [1] in order to achieve optimum contrast for the ferritin label.

Identification of Lectin Binding Sites

At the electron microscopic level of investigation the fused cells are characterized by the appearance of vacuoles of varying size and large numbers of transsection profiles of auto- and heterophagic vacuoles and "lipid-like droplets" (Fig. 6*a*). In addition, clusters of membranes can be detected in all parts of the fused cell. Typical is the occurrence of stack-like membrane clusters in the regions close to the surrounding plasma membrane (Fig. 6*a*). In both series of experiments using either Con A-gold and succinyl Con A-ferritin or PNA-HRP and succinyl Con A-ferritin both labels can be recovered at the surrounding plasma membrane in close vicinity (Fig. 6*b* and *c*). Furthermore, ferritin, HRP or gold coupled lectins are recovered intracellularly (Fig. 6*e* and *f*). Although their locations vary, most of the markers are found within heterophagic vacuoles and at membranes of endocytic vesicles, at internalized membrane clusters and within lysosomal structures. The co-localization of gold- and ferritin-labeled lectins as well as of HRP- and ferritin-labeled lectins at the surrounding plasma membrane and in auto- and heterophagic vacuoles of fused MDCK cells proves the event of cell fusion. The drastically enhanced vacuolization found in fused cells must be considered as a consequence of enhanced internalization of plasma membrane portions during the fusion process. Furthermore, this process seems to be accompanied by an enhanced turnover of cellular compounds illustrated by the high frequency of auto- and heterophagic vacuoles (Fig. 6*a* and *c*) as well as by the large numbers of coated pits (Fig. 6*b*). Electron-dense markers not associated with membrane structures but located within membrane-demarcated vacuoles result from lysosomal degrada-

Fig. 4. Single and fused cells marked by fluorescence-labeled peanut lectins. The length of the bars indicates 50 μm. (*A*) Single cells marked with either FITC (open arrows) or Rhodamine (solid arrows) labeled peanut lectins using interference contrast microscopy. (*B*) The same cells as shown at left but double exposed to two different excitation wave-lengths: 450–490 nm, FITC-label visible (green), open arrows; 510–560 nm, Rhodamine-label visible (red), solid arrows. (*C*) Cell aggregation of Rhodamine (solid arrows) and FITC (open arrows) marked single cells 30 min after PEG treatment (interference contrast). (*D*) The same cell aggregation as shown at left but double exposed to the two excitation wave-lengths mentioned above. (*E*) Cell aggregation of FITC or Rhodamine marked cells 60 min after PEG treatment. Single cell borders are still visible (arrows), but plasma membranes are increasingly mixed. Thus, monochromatic green and red light results in a yellowish emission of light. (*F*) Fused cell 120 min after PEG treatment. No single cell borders are detectable. No labels are visible in the plasma membrane of the "giant" cell. Both markers are rather equally dispersed in the cytoplasmic compartment of the fused cell. This results in an almost homogeneous yellowish emission of light

Fig. 5. Fate of single cell nuclei in polynucleated homokaryons. Length of bars indicates 50 μm. (*A*) Single cells and small fused cells one day after PEG treatment. The cell borders of a single cell are marked by open arrows. The cell nucleus in this single cell and two couples of nuclei in two fused cells are marked with solid arrows. (*B*) A "giant" fused cell one day after PEG treatment. The cell borders of the fused cell are marked with open arrows. One cell nucleus in the fused cell is marked with a short solid arrow. Two cell nuclei of two single, nonfused MDCK cells are marked with long solid arrows. (*C* and *D*) Cell nuclei in fused cells seven days (*C*) and 10 days (*D*) after PEG treatment. (*E*) One "giant" fused cell 21 days after PEG treatment. Cell borders of this fused cell are marked with open arrows. The size of the cell nucleus in the fused cell (X) is clearly increased as compared to single cell nuclei (solid arrows)

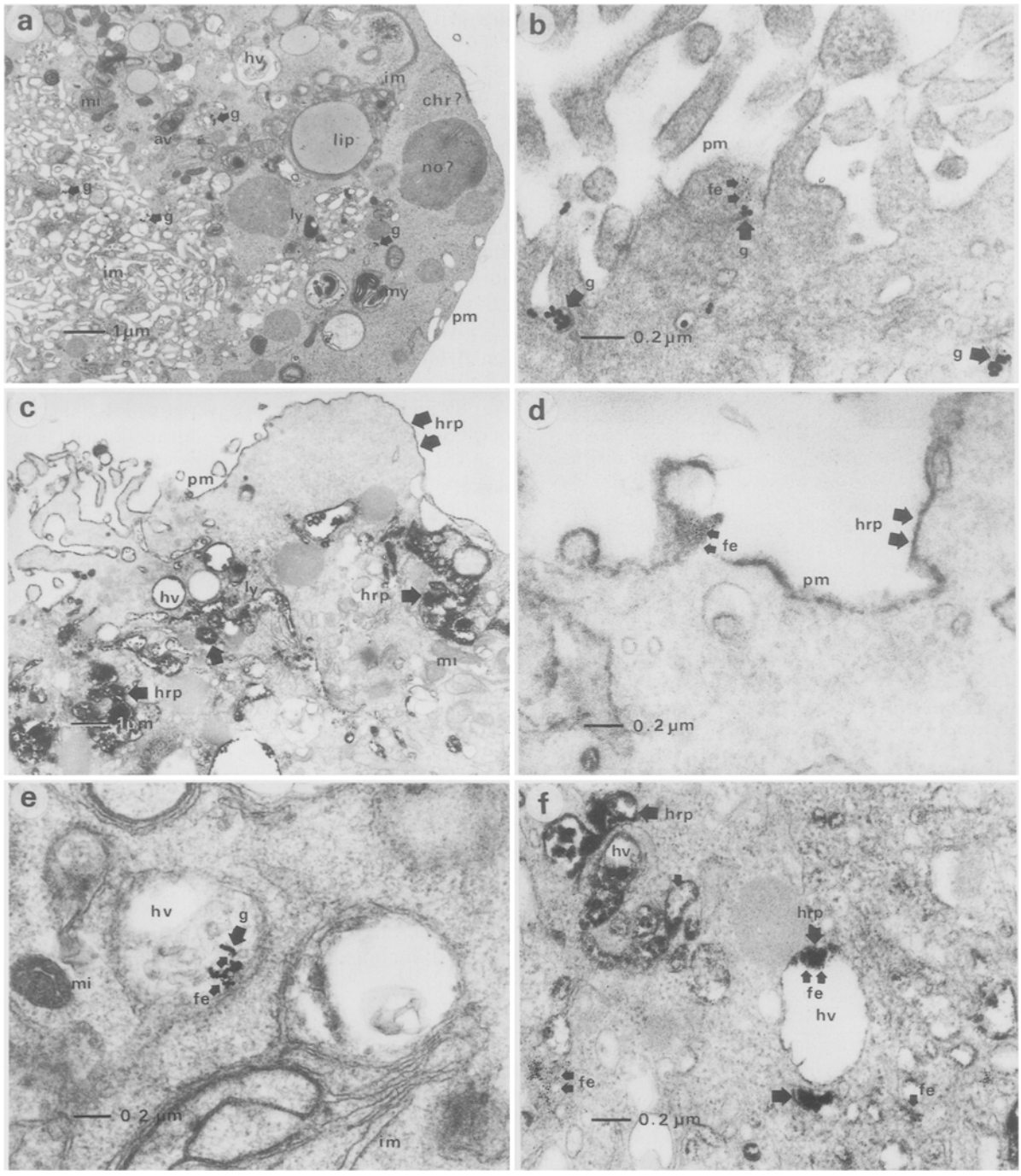

Fig. 6. Lectin binding to MDCK cells 120 min after fusion by PEG. (*a*) Low magnification electron micrograph of a fusion aggregate. The surrounding plasma membrane is fairly smooth and does not display microvillar structures. Within the cytoplasmic compartment numerous vacuoles, auto- and heterophagic structures and internalized membranes, presumably resulting from internalization processes during cell fusion, can be detected. Arrows indicate internalized gold particles (15 nm) covalently coupled to Con A. The ferritin label coupled to succinyl Con A cannot be detected at this level of magnification. *av*: autophagic vacuoles; *chr*: chromatin; *g*: gold particles; *hv*: heterophagic vacuoles; *im*: internalized membranes; *lip*: liposomal structures; *ly*: lysosome; *mi*: mitochondria; *my*: myelin figures in auto- or heterophagic vacuoles; *no*: nucleolus; *pm*: surrounding plasma membrane. (*b*) Higher magnification of a fused cell aggregate labeled with Con A-gold and succinyl Con A-ferritin. The region depicted shows a portion of the surrounding plasma membrane, bearing several microvilli. Both labels are marked by arrows. Con A-gold is recovered at the membrane of microvilli as well as in coated pits, which indicates an endocytic uptake route. At the same membrane and in close vicinity to Con A-gold, the ferritin labeled succinyl Con A can also be easily recognized (small arrows). In the lower right corner endocytosed markers can be seen. *fe*: ferritin particles; *g*: gold particles; *pm*: surrounding plasma membrane. (*c*) Low magnification electron micrograph of fused MDCK

tion. Although no histochemical reaction for acid hydrolases has been carried out, it is likely that these vacuoles are lysosomes. Quite frequently regions with a disintegrated nuclear envelope can be found. Nucleoli and euchromatin are found freely dispersed in the cytoplasmic compartment. These findings can be explained by degradation of single-cell nuclei in the fused cell.

The lectin labeling pattern of membranes differs with respect to the type of lectins used. The far lower labeling density obtained with gold- and ferritin-coupled Con A as compared to HRP labeled PNA may reflect a larger number of membrane glycoproteins with reactive D-galactose instead of D-mannose moieties. The fairly homogeneous distribution of PNA-HRP along the membranes probably is a result of the presence of the ganglioside GN1 in the MDCK plasma membrane, which amounts 5% of all gangliosides present in MDCK cells [19].

Discussion

Future Aspects of Epithelial Cell Fusion

We have developed this fusion technique with the goal to produce rather large but still viable polynucleated homokaryons. We have shown that plasma membrane is externalized when a MDCK monolayer is trypsinized and internalized when cells are fused. Furthermore, from the fact that the number of nuclei in polynucleated cells decreases with time while the size of the nuclei increases we derive that nuclear fusion occurs with a lag period of several days after fusion. The following paper [21] deals with aldosterone action in MDCK cells, employing cytoplasmic pH and cell membrane conductance measurements simultaneously, feasible only in a "giant" MDCK cell. We are quite confident that the fusion technique described can be applied also to other epithelial and nonepithelial established cell lines and primary cell cultures. Recently we have fused MDCK cells with a primary culture of respiratory epithelium, resulting in polynucleated heterokaryons. With such techniques it should be possible in the future to immortalize specific cell functions of a primary cell culture by fusing its genetic material into an immortal cell as the MDCK cell. Nevertheless, cell growth and cell division of such epithelial heterokaryons are the basic prerequisites for further studies that have not yet been tested.

We thank Drs. S. Silbernagl and J. Schwegler for their encouraging discussions during the course of this study. H. Joha performed the experiments on fluorescent lectins in partial fulfillment of the requirements of his M.D. thesis. The project was supported by the Deutsche Forschungsgemeinschaft, SFB 176, A6. We gratefully acknowledge the generous financial support for the publication of Figs. 4 and 5 by Carl Zeiss Co., Oberkochen, FRG.

References

1. Ainsworth, S.K., Karnovsky, M.J. 1972. An ultrastructural staining method for enhancing the size and electron opacity of ferritin in thin sections. *J. Histochem. Cytochem.* **20:**225–228
2. Berridge, M.J., Irvine, R.F. 1984. Inositol trisphosphate, a novel second messenger in cellular signal transduction. *Nature (London)* **312:**315–321
3. Bouachour, G., Planelles, G., Anagnostopoulos, T. 1988. Fusion of amphibian proximal convoluted cells into giant cells. *Pfluegers Arch.* **411:**220–222
4. Boulpaep, E.L. 1976. Electrical phenomena in the nephron. *Kidney Int.* **9:**88–102
5. Cereijido, M., Ehrenfeld, J., Fernandez-Castelo, S., Meza, I. 1981. Fluxes, junctions, and blisters in cultured monolayers of epithelioid cells (MDCK). *Ann N.Y. Acad. Sci.* **372:**422–441
6. Dietl, P., Wang, W., Oberleithner, H. 1987. Fused cells of frog proximal tubule: I. Basic membrane properties. *J. Membrane Biol.* **100:**43–51
7. Frömter, E. 1984. Viewing the kidney through microelectrodes. *Am. J. Physiol.* **247:**F695–F705
8. Giebisch, G. 1987. Transport of electrolytes across renal tubules. *In:* Renal Physiology: People and Ideas. C.W. Gottschalk, R.W. Berliner and G.H. Giebisch, editors. pp. 165–216. American Physiological Society, Bethesda, MD
9. Graham, R.C., Karnovsky, M.J. 1966. The early stage of absorption of injected horseradish peroxidase in the proximal tubules of mouse kidney: Ultrastructural cytochemistry by a new technique. *J. Histochem. Cytochem.* **14:**291–302
10. Handler, J.S., Perkins, F.M., Johnson, J.P. 1980. Studies of renal cell function using cell culture techniques. *Am. J. Physiol.* **238:**F1–F9
11. Hannun, Y.A., Bell, R.M. 1988. Aminoacridines, potent inhibitors of protein kinase C. *J. Biochem. Chem.* **263:**5124–5131
12. Harris, H., Watkins, J.F. 1965. Hybrid cells derived from mouse and man: Artificial heterokaryons of mammalian cells from different species. *Nature (London)* **205:**640–646

cells prelabeled with PNA-HRP and succinyl Con A-ferritin. Again, no ferritin label is visible at this level of magnification. However, HRP-labeled surrounding plasma membrane as well as internalized HRP-bearing membrane portions can be clearly identified (arrows). As in endocytic vacuoles and heterophagic structures containing the HRP label are present. *hrp*: horseradish peroxidase coupled to PNA: *hv*: heterophagic vacuoles; *ly*: lysosomes; *mi*: mitochondria; *pm*: surrounding plasma membrane. (*d*) Higher magnification of *c*. Both HRP and ferritin conjugated lectins are found on the same plasma membrane of a fused cell aggregate. *fe*: succinyl Con A-ferritin; *hrp*: HRP-PNA; *pm*: surrounding plasma membrane. (*e* and *f*) Electron micrographs at higher magnification displaying heterophagic vacuoles in the cytoplasm of fused MDCK cells with internalized membrane labels. *e*: ferritin and gold; *f*: ferritin and HRP

13. Holthöfer, H., Virtanen, I., Pettersson, E., Törnroth, T., Alfthan, O., Linder, E., Miettinen, A. 1981. Lectins as fluorescence microscopic markers for saccharides in the human kidney. *Lab. Invest.* **45:**391–399
14. Karst, W., Merker, H.J. 1988. The differentiation behaviour of MDCK cells grown on matrix components and in collagen gels. *Cell Differ.* **22:**211–224
15. Knutton, S. 1979. Studies of membrane fusion: III. Fusion of erythrocytes with polyethylene glycol. *J. Cell. Sci.* **36:**61–72
16. Köhler, G., Milstein, C. 1975. Continuous cultures of fused cells secreting antibody of predefined specificity. *Nature (London)* **256:**495–497
17. Le Hir, M., Dubach, U.C. 1982. The cellular specificity of lectin binding in the kidney: II. A light microscopical study in the rabbit. *Histochemistry* **74:**531–540
18. Madin, S.H., Darby, N.B., Jr. 1958. CCL-34, *as cataloged in:* American Type Culture collection Catalogue of Strains. H.O. Hatt, editor. 1975, Vol. 2, p. 47. Library of Congress, Rockville, Maryland
19. Markwell, M.A.K., Fredman, P., Svennerholm, L. 1984. Receptor ganglioside content of three hosts for sendai virus: MDBK, Hela and MDCK cells. *Biochim. Biophys. Acta* **775:**7–16
20. Nelson, W.J., Veshnock, P.J. 1987. Modulation of fodrin (membrane skeleton) stability by cell-cell contact in Madin Darby canine kidney epithelial cells. *J. Cell Biol.* **104:**1527–1537
21. Oberleithner, H., Kersting, U., Silbernagl, S., Steigner, W., Vogel, U. 1989. Fusion of cultured dog kidney (MDCK) cells: II. Relationship between cell pH and K^+ conductance in response to aldosterone. *J. Membrane Biol.* **111:**49–56
22. Oberleithner, H., Schmidt, B., Dietl, P. 1986. Fusion of renal epithelial cells: A model for studying cellular mechanisms of ion transport. *Proc. Natl. Acad. Sci. USA* **83:**3547–3551
23. Oberleithner, H., Weigt, M., Westphale, H.J., Wang, W. 1987. Aldosterone activates Na^+/H^+ exchange and raises cytoplasmic pH in target cells of the amphibian kidney. *Proc. Natl. Acad. Sci. USA* **84:**1464–1468
24. Paulmichl, M., Gstraunthaler, G., Lang, F. 1985. Electrical properties of Madin-Darby canine kidney cells. Effects of extracellular potassium and bicarbonate. *Pfluegers Arch.* **405:**102–107
25. Rindler, M.J., Chuman, L.M., Shaffer, L., Saier, M.H., Jr. 1979. Retention of differentiated properties in an established dog kidney epithelial cell line (MDCK). *J. Cell Biol.* **81:**635–648
26. Roos, D.S., Davidson, R.L., Choppin, P.W. 1987. Control of membrane fusion in polyethylene glycol-resistant cell mutants: Applications to fusion technology. *In:* Cell Fusion. A.E. Sowes, editor. pp. 123–144. Plenum, New York
27. Saier, M.H., Jr. 1981. Growth and differentiated properties of a kidney epithelial cell line (MDCK). *Am. J. Physiol.* **240:**C106–C109
28. Seglen, P.O. 1973. Preparation of rat liver cells: II. Effects of ions and chelators on tissue dispersion. *Exp. Cell Res.* **76:**25–30
29. Simmons, K. 1987. Membrane traffic in an epithelial cell line derived from the dog kidney. *Kidney Int.* **32:**201–207
30. Simmons, N.L. 1984. Epithelial cell volume regulation in hypotonic fluids: Studies using a model tissue culture renal epithelial cell system. *Q. J. Exp. Physiol.* **69:**83–95
31. Spring, K.R. 1985. The study of epithelial function by quantitative light microscopy. *Pfluegers Arch.* **405:**S23–S27
32. Stewart, W.W. 1981. Lucifer dyes—highly fluorescent dyes for biological tracing. *Nature (London)* **292:**17–21
33. Taub, M. 1985. Importance of hormonally defined, serum-free medium for in vitro studies concerning epithelial transport. *In:* Tissue Culture of Epithelial Cells. M. Taub, editor, pp. 255–276. Plenum, New York
34. Wang, W., Wang, Y., Silbernagl, S., Oberleithner, H. 1988. Fused cells of frog proximal tubule: II. Voltage-dependent intracellular pH. *J. Membrane Biol.* **101:**259–265
35. Westerwoudt, R.J. 1985. Improved fusion methods: IV. Technical aspects. *J. Immunol. Methods* **77:**181–196
36. Willingham, M.C., Rutherford, A.V. 1984. The use of osmium-thiocarbohydrazide-osmium (OTO) and ferrocyanide-reduced osmium methods to enhance membrane contrast and preservation in cultured cells. *J. Histochem. Cytochem.* **32:**455–460
37. Windhager, E.E. 1987. Micropuncture and microperfusion. *In:* Renal Physiology: People and Ideas. C.W. Gottschalk, R.W. Berliner, and G.H. Giebisch, editors. pp. 101–129. American Physiological Society, Bethesda, MD
38. Zimmermann, V., Vienken, J. 1982. Electric field-induced cell-to-cell fusion. *J. Membrane Biol.* **67:**165–182

Received 23 August 1988; revised 3 January 1989